Cancer Cell, Volume *34*

Supplemental Information

Epidermal Growth Factor Receptor Extracellular Domain Mutations in Glioblastoma Present Opportunities for Clinical Imaging and Therapeutic Development

Zev A. Binder, Amy Haseley Thorne, Spyridon Bakas, E. Paul Wileyto, Michel Bilello, Hamed Akbari, Saima Rathore, Sung Min Ha, Logan Zhang, Cole J. Ferguson, Sonika Dahiya, Wenya Linda Bi, David A. Reardon, Ahmed Idbaih, Joerg Felsberg, Bettina Hentschel, Michael Weller, Stephen J. Bagley, Jennifer J.D. Morrissette, MacLean P. Nasrallah, Jianhui Ma, Ciro Zanca, Andrew M. Scott, Laura Orellana, Christos Davatzikos, Frank B. Furnari, and Donald M. O'Rourke

Table S1. Related to Table 1. Patient demographics of the discovery GBM cohort at UPenn.

Variable		n	%
Gender	Female	103	40
	Male	157	60
Age (year)	0-29	2	1
	30-49	26	10
	50-69	157	60
	70+	75	29
MGMT	Unmethylated	122	47
	Methylated	87	33
	Unknown	51	20
EGFR	Non-Amplified	162	62
	Amplified	98	38
EGFRvIII	Negative	154	59
	Postive	50	19
	Unknown	56	22
Misense Mutants	A289D/T/V	15	6
	R108G/K	9	3
	G598V	6	2

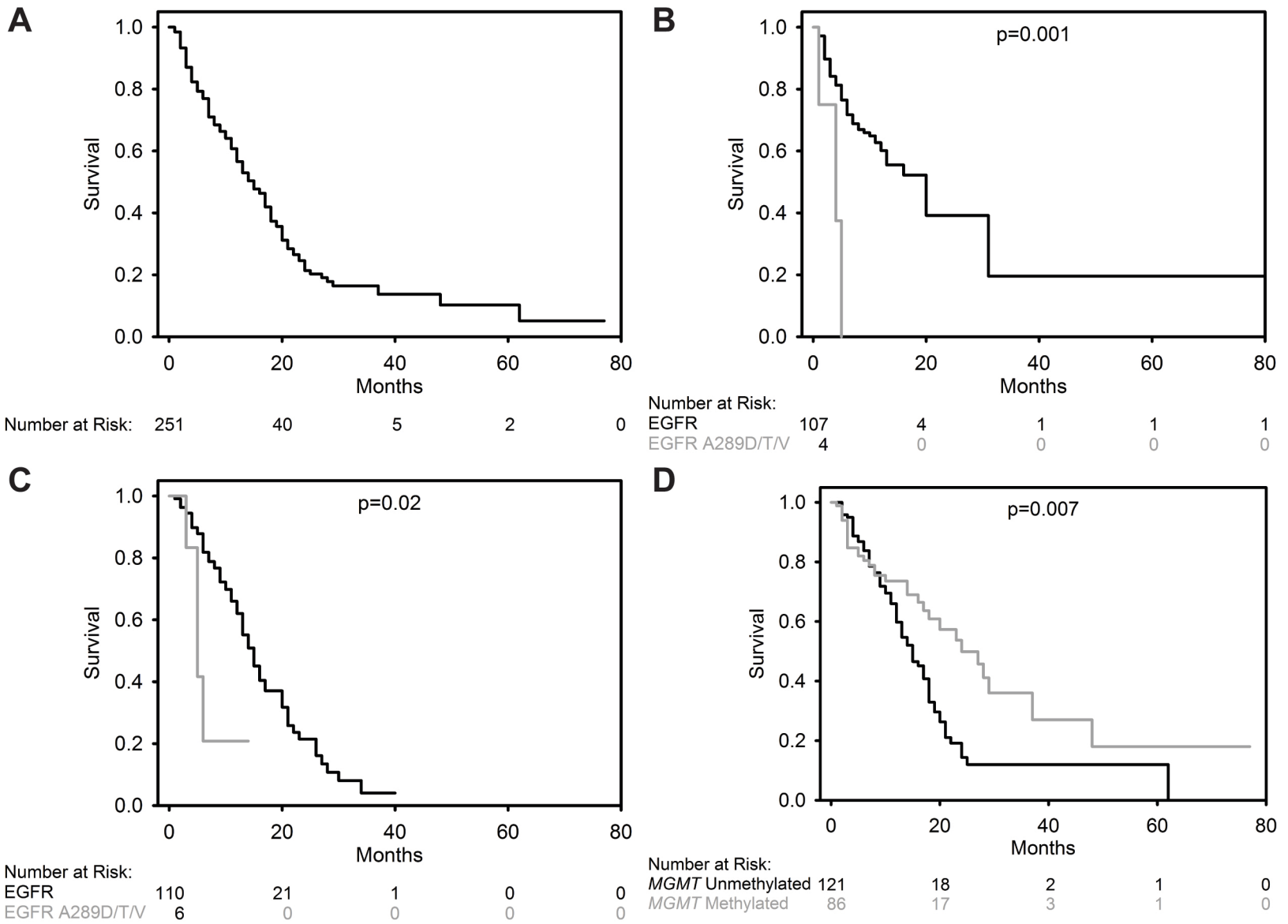

Figure S1. Related to Figure 1. (A-D) Kaplan-Meier survival curves for the total cohort of 260 *IDH1* wildtype, de novo GBMs (A), the validation UPenn cohort (B), the validation French cohort (C), and *MGMT* methylated versus MGMT unmethylated GBM patients (D).

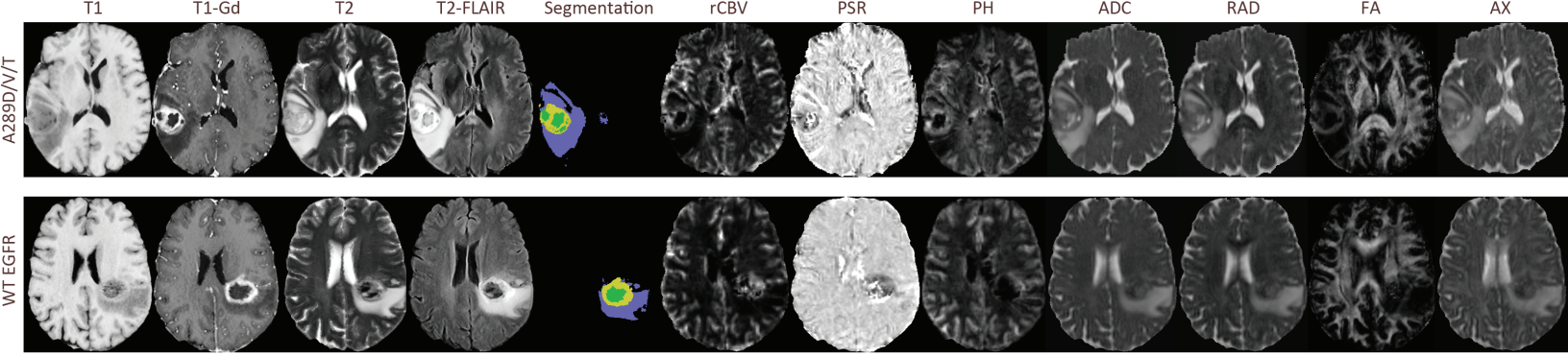

Figure S2. Related to Figure 2. Representative images for the basic and advanced imaging modalities included in the final analyses. Abbreviations: T1-Gd=T1-weighted MRI with gadolinium; T2-FLAIR=T2-weighted fluid Attenuated Inversion Recovery MRI; rCBV=relative cerebral blood volume; PSR=percentage signal recovery; PH=peak height; ADC=apparent diffusion coefficient; RAD=radial diffusivity; FA=fractional anisotropy; AX=axial diffusivity.

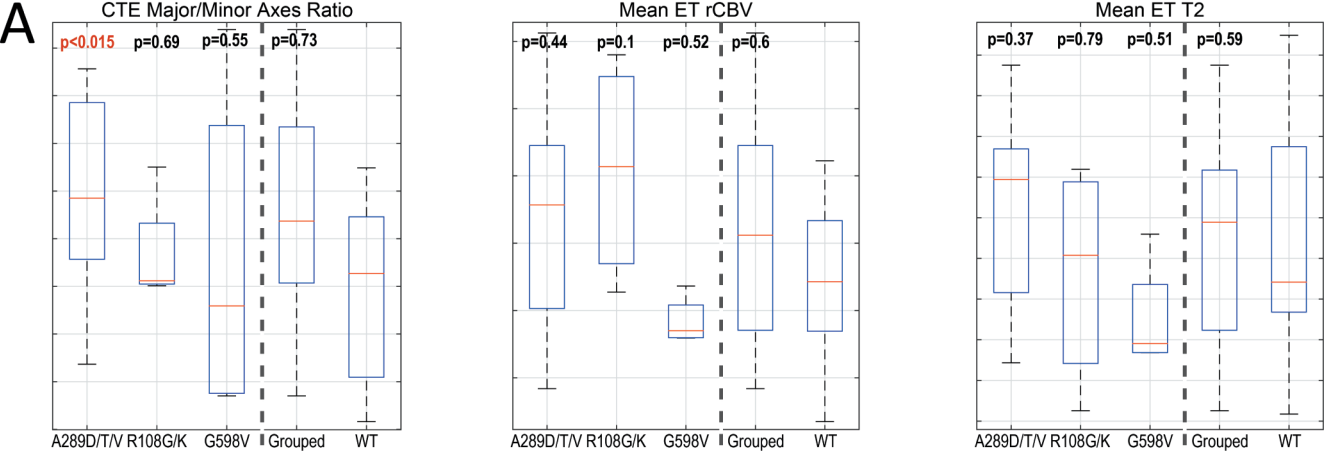

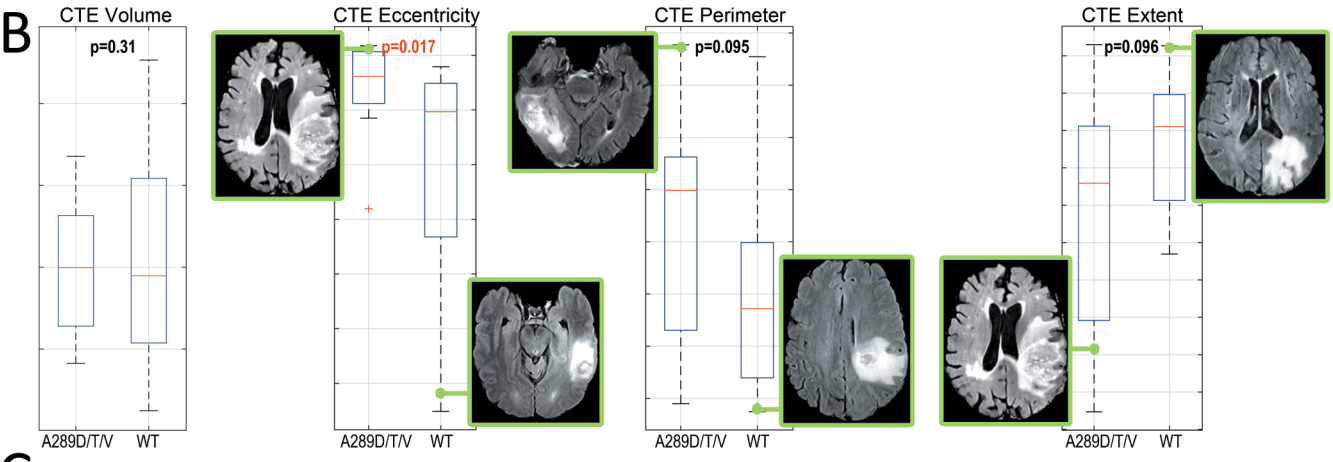

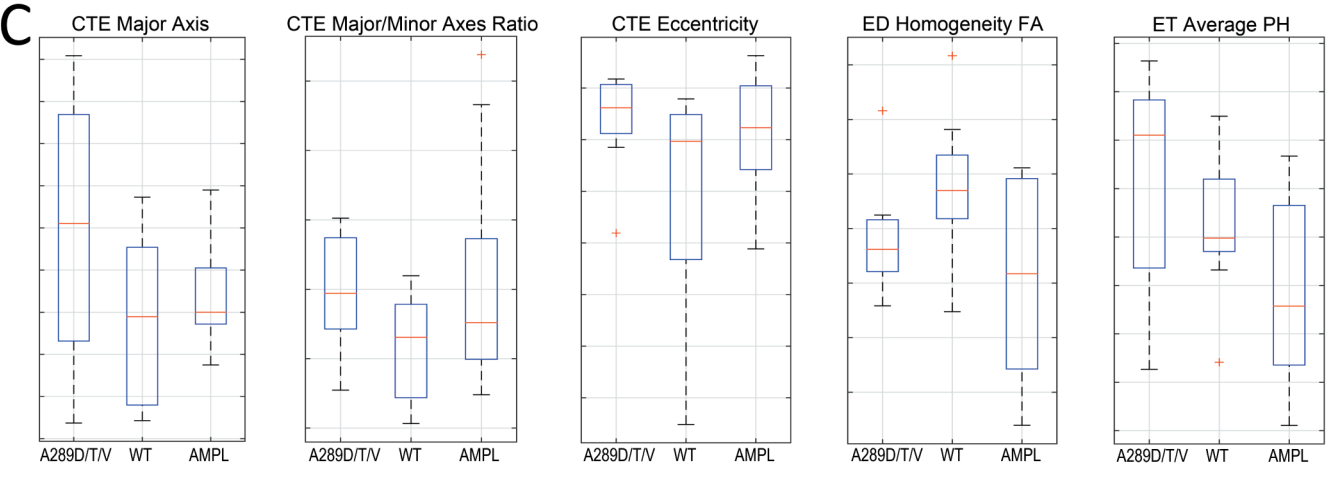

D

	CTE Major Axis	CTE Major/Minor Axes Ratio	CTE Eccentricity	ED Homogeneity FA	ET Average PH
A289D/T/V vs AMPL	0.0844	**0.0086**	**0.0215**	0.3007	**0.0221**
A289D/T/V vs WT	0.7702	0.0605	**0.0375**	**0.0444**	0.1519
WT vs AMPL	0.0669	0.9865	0.4943	**0.0141**	0.0899

Figure S3. Related to Figure 2. (A) Feature comparison across each individual EGFR missense mutation, the grouped mutations, and WT EGFR, for the major: minor axes ratio of the CTE (left), the average rCBV signal in the ET (middle), and the average T2 signal in the ET (right). P-values represent each condition versus WT EGFR. (B) While the volume distribution of the CTE is similar between the $EGFR^{A289D/T/V}$ and the WT EGFR cohorts, the higher eccentricity and perimeter values, combined with lower extent values, in the $EGFR^{A289D/T/V}$ cohort present a picture of more irregularly-shaped tumors, suggestive of more invasive tumors. Insets show representative T2-FLAIR MRI examples of both $EGFR^{A289D/T/V}$ and WT EGFR tumors demonstrating corresponding plotted features. (C) Comparison across $EGFR^{A289D/T/V}$, WT EGFR, and EGFR-amplified patients. $EGFR^{A289D/T/V}$ mutant cases demonstrated distinct distributions from the other two populations, with the exception of the homogeneity in the FA signal of the ED region. (D) Two-sided T test p values for the features in plotted in (C). Feature definitions: The “Eccentricity” defines the circularity of the assessed shape, i.e. eccentricity value of 0 describes a perfect circle and larger values represent more elongated shapes. The “Perimeter” describes the distance around the boundary of the assessed shape. The “Extent” is the ratio of the area of the assessed shape to the area of its rectangular bounding box. The top and bottom of each “box” depict the 3rd and 1st quartile of the represented measure, respectively, whereas the red line within each box indicates the median value. The fact that these are not necessarily at the center of each box indicates the skewness of the distribution over different cases. The “whiskers” drawn above and below each box depict the extremal observations still within 1.5 times the interquartile range, above the 3rd or below the 1st quartile. Observations beyond the whiskers are marked as outliers with a “+” sign.Abbreviations: CTE=complete tumor extent; ET=enhancing tumor; rCBV=relative cerebral blood volume; ED=peritumoral edematous/invaded region; FA=fractional anisotropy; PH=peak height.

Table S3, related to Figure 2. Selected quantitative imaging phenomic features.

EGFR alteration	Tumor sub-region	Feature Observation	p value
R108G/K vs A289D/T/V	NET	higher T1	0.0029
R108G/K vs WT EGFR	ET	higher Peak Height (measurement extracted from perfusion - DSC-MRI)	0.0276
R108G/K vs WT EGFR	ED	lower Homogeneity in the Fractional Anisotropy signal	0.0487
A289D/T/V vs WT EGFR	ED	lower Homogeneity in the Fractional Anisotropy signal	0.0283
R108G/K vs WT EGFR	NET	higher standard deviation (i.e. more variance) in the Peak Height signal	0.0485
A289D/T/V vs WT EGFR	NET	higher standard deviation (i.e. more variance) in the Peak Height signal	0.0309
G598V vs WT EGFR	ET	lower average T1 signal	0.0125
A289D/T/V vs WT EGFR	ET	lower average T1 signal	0.0081
A289D/T/V vs WT EGFR	CTE	Major/Minor Axis	0.0149
G598V vs WT EGFR	ET	higher relative enhancement (T1Gd-T1)	0.0326
A289D/T/V vs WT EGFR	ET	higher relative enhancement (T1Gd-T1)	0.0374
G598V vs WT EGFR	ED	higher relative enhancement (T1Gd-T1)	0.0026
A289D/T/V vs WT EGFR	ED	higher relative enhancement (T1Gd-T1)	0.0441
A289D/T/V vs WT EGFR	NET	higher relative enhancement (T1Gd-T1)	0.0236
A289D/T/V vs WT EGFR	CTE	longer Major Axis	0.0064
A289D/T/V vs WT EGFR	CTE	higher Eccentricity	0.0176

The described feature observations are the ones denoted as statistically significant ($p \leq 0.05$), based on the applied multivariate approach for feature selection (Gaonkar and Davatzikos, 2013) and after selection based on radiographic interpretation. Furthermore, this table denotes the tumor sub-regions in which each of these feature observations were captured, as well as the pairs of EGFR variants that these features were found as statistically significant.Abbreviations: ED, peritumoral edematous/infiltrated tissue; ET, enhancing part of tumor core; NET, non-enhancing part of tumor core; CTE, complete tumor extent, encompassing of all ET, NET, and ED; Tumor core, typically resected tumor.

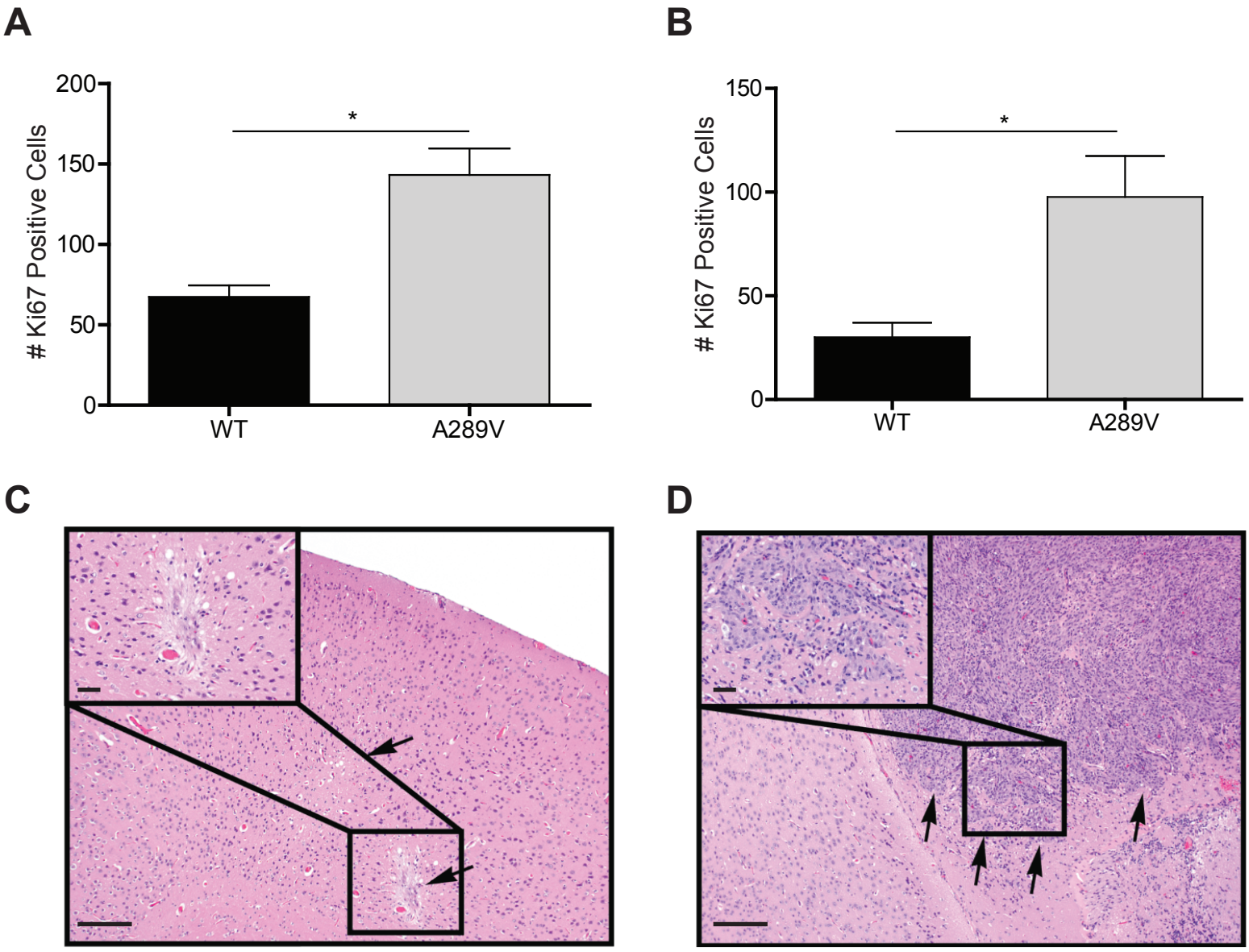

Figure S4. Related to Figure 3. (A and B) Quantification of Ki67 positive cells from U87 tumors from Figure 3C (A) and HK281 tumors from Figure 3D (B). Error bars indicate +/- standard error of the mean. (C and D) H&E images at Day 14 of animals injected with U87 WT EGFR (C) and U87 $EGFR^{A289V}$ (D). The WT EGFR demonstrated scar tissue from the needle track and a small focus of tumor cells (arrows and insert). The $EGFR^{A289V}$ missense mutation formed a densely cellular invasive growth effacing and infiltrating unilaterally the frontal cortex (arrows and insert). Scale bar low magnification = 170 μm. Scale bar high magnification = 70 μm.

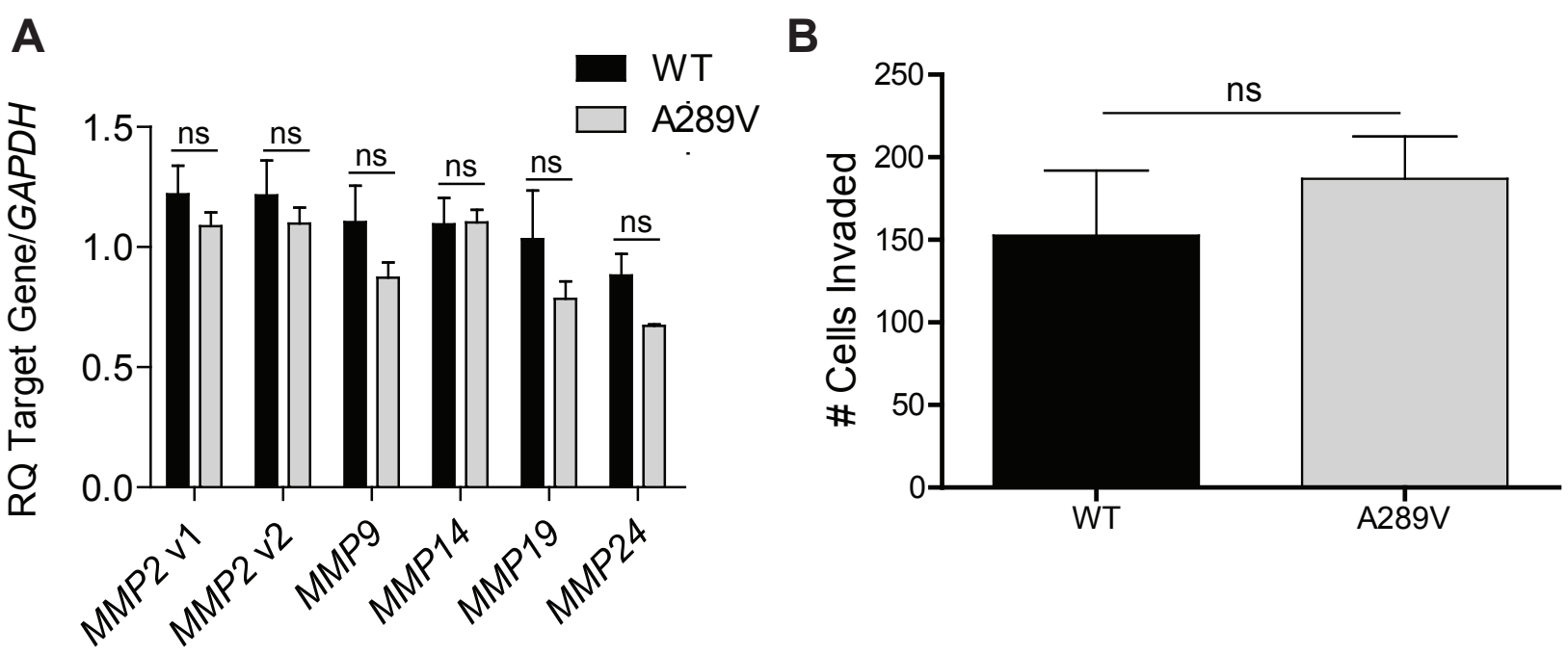

Figure S5. Related to Figure 4. Effect of EGFR^{A289V} on *MMP* expression. (A) Real time quantitative PCR analysis of *MMP2*, *MMP9*, *MMP14*, *MMP19*, and *MMP24* in U87 glioma cells expressing either WT EGFR or EGFR^{A289V}. Data shown are fold change gene expression relative to *GAPDH*. (B) Quantification of invaded U87 glioma cells was determined using a modified Boyden Transwell chamber assay coated with matrigel. Error bars are standard error of the mean of at least three replicates and represent at least three independent experiments. ns = not significant.

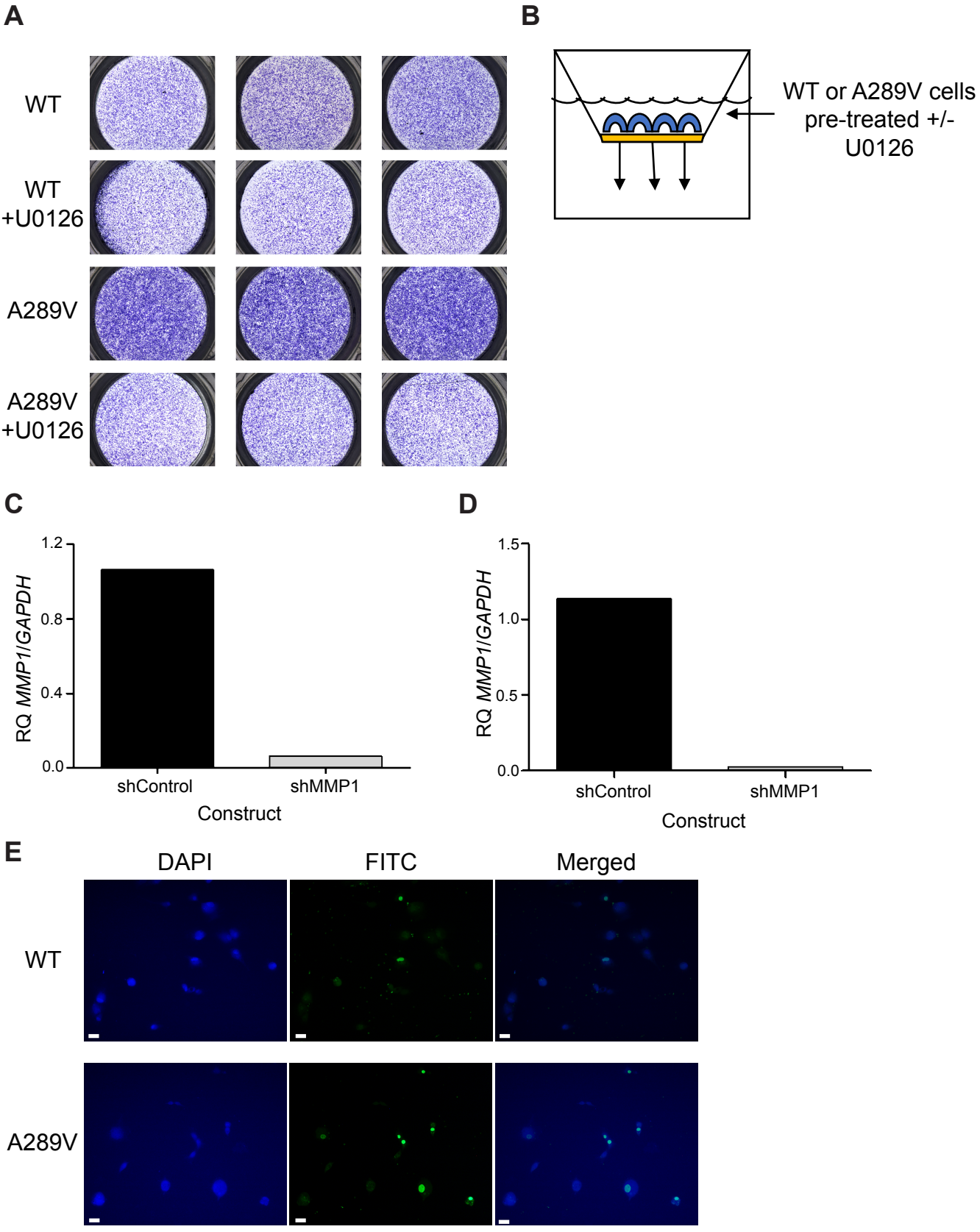

Figure S6. Related to Figure 5. (A) Representative images from Figure 5C showing crystal violet stained HK281 GBM-spheres post-invasion. (B) Schematic of basic experimental set-up using modified Boyden Transwell chambers. (C and D) Real time quantitative PCR analysis of *MMP1* in EGFR^{A289V} expressing U87 glioma cells (C) and HK281 GBM-spheres (D) transduced with shMMP1 or shControl. Data shown are fold change gene expression relative to *GAPDH*. (E) Representative images showing Hoechst and BrdU stained U87 WT EGFR (top) and U87 A289V (bottom) following BrdU incorporation. Scale bar = 22 μm.

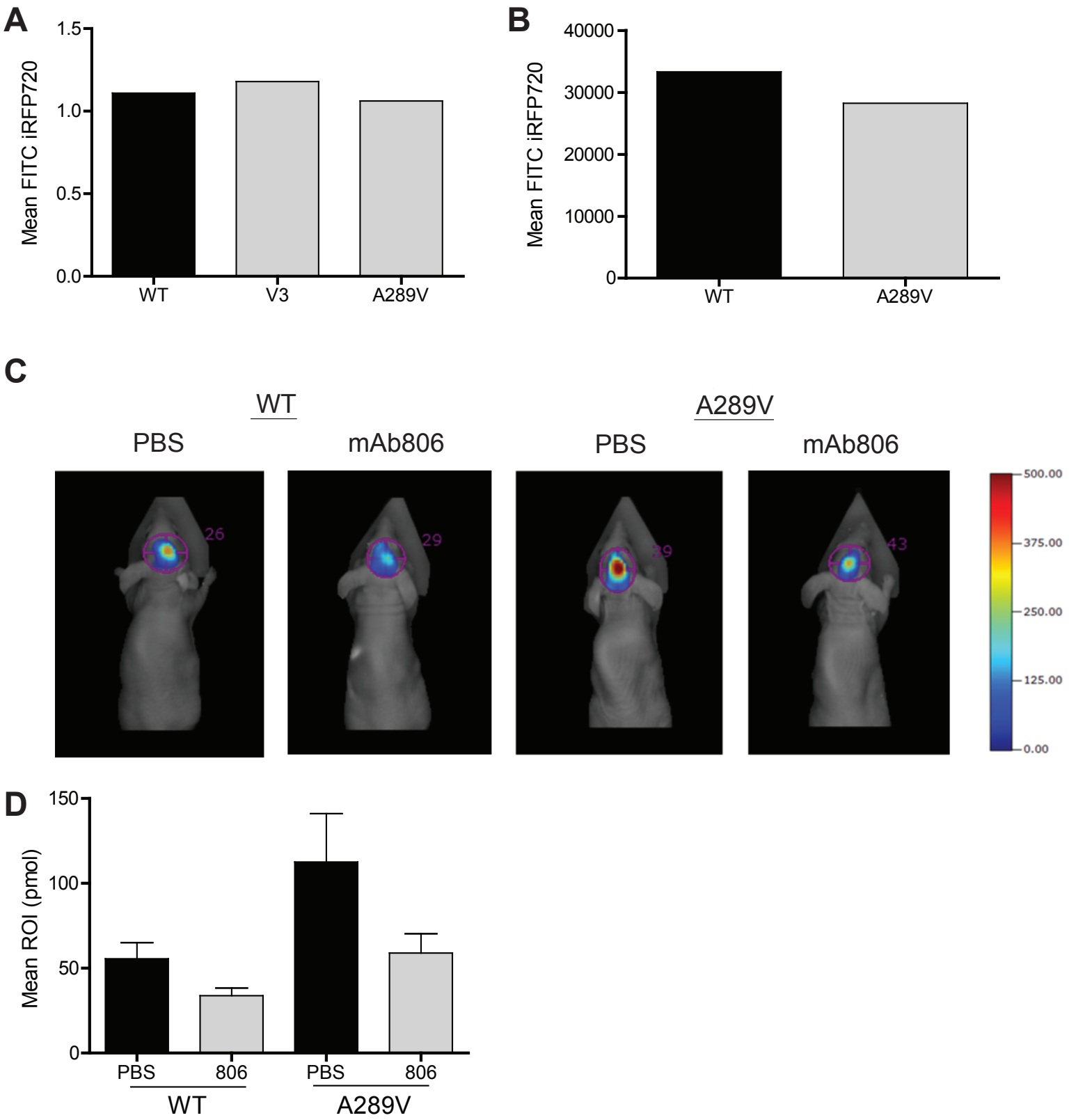

Figure S7. Related to Figure 6. (A and B) Flow cytometric analyses of U87-iRFP720 glioma cells (A) and HK281-iRFP720 GBM-spheres (B) expressing WT EGFR, EGFRvIII (V3), or EGFR^{A289V}. (C) Representative images of HK281-iRFP720-expressing tumors as detected by fluorescence molecular topography (FMT) as described in Figure 6. (D) Quantification of FMT signal intensity on Day 12 post-implantation for each region of interest. Error bars are standard error of the mean.

Table S4. Related to STAR Methods. Patient MRI specifics.

	Dimensions (pixels)	Spatial Resolution (mm^3)	Slice Spacing (mm)	TI (ms)	TR (ms)	TE (ms)
T1	192x256x192	0.976x0.976x1	1	950	1760	3.1
T1Gd	192x256x192	0.976x0.976x1	1	950	1760	3.1
T2	208x256x64	0.938x0.938x3	3		4680	85
T2-FLAIR	192x256x64	0.938x0.938x3	3	2500	9420	141
DSC-MRI	128x128x20	1.72x1.72x3	3		2000	45
DTI	128x128x40	1.72x1.72x3	3		5000	86

Table S5. Related to STAR Methods. Real time PCR primer sequences.

Primer Name	Forward	Reverse
MMP1	GGTCTCTGAGGGTCAAGCAG	AGTTCATGAGCTGCAACACG
MMP2 v1	GGAGTACTGCAAGTTCCCCT	TCAGTGGTGCAGCTGTCATA
MMP2 v2	GGAGTACTGCAAGTTCCCCT	TCAGTGGTGCAGCTGTCATA
MMP9	GAGACTCTACACCCAGGACG	GAAAGTGGGGAAGACGC
MMP14	GCTGCCTACCGACAAGATTG	TTCATCGCTGCCCATGAATG
MMP19	CAGCCTCGTTGTGGCCTAGA	ACCAGCCTGCACCTCTTGGA
MMP24	GAACCTGTGGGCAAGACCTA	TGACAACCAGAAACTGAGCG
GAPDH	AAATCCCATCACCATCTTCCAGGAGC	CATGGTTCACACCCATGACGAACA

Abbreviations: MMP, Matrix Metalloproteinase; GAPDH, glyceraldehyde-3-phosphate dehyrodgenase.